

**Title: Network Analysis Prioritizes DEWAX and ICE1 as the Candidate Genes for Major eQTL Hotspots in Seed Germination of *Arabidopsis thaliana***

**Author names and affiliations**

Margi Hartanto<sup>\*</sup>, Ronny V. L. Joosen<sup>†</sup>, Basten L. Snoek<sup>‡</sup>, Leo A. J. Willems<sup>†</sup>, Mark G. Sterken<sup>§</sup>, Dick de Ridder<sup>\*</sup>, Henk W. M. Hilhorst<sup>†</sup>, Wilco Ligterink<sup>†</sup>, Harm Nijveen<sup>\*,\*\*</sup>

<sup>\*</sup>Bioinformatics Group, Wageningen University, NL-6708 PB Wageningen, The Netherlands

<sup>†</sup>Laboratory of Plant Physiology, Wageningen University, NL-6708 PB Wageningen, The Netherlands

<sup>‡</sup>Theoretical Biology and Bioinformatics, Utrecht University, 3584 CH Utrecht, The Netherlands

<sup>§</sup>Laboratory of Nematology, Wageningen University, NL-6708 PB Wageningen, The Netherlands

**Data availability**

Cel files of microarray data have been deposited in the ArrayExpress database at EMBL-EBI ([www.ebi.ac.uk/arrayexpress](http://www.ebi.ac.uk/arrayexpress)) under accession number E-MTAB-9080. The code for the analysis and visualization is available in the form of R scripts at the Wageningen University GitLab repository (<https://git.wur.nl/harta003/seed-germination-qtl>).

**Running title: eQTL hotspots in seed germination**

**Keywords:** Arabidopsis, eQTL, network analysis, seed germination.

**Corresponding authors:**

Margi Hartanto, Droevendaalsesteeg 1 6708PB WAGENINGEN, phone number:  
+31630634476, email: [margi.hartanto@wur.nl](mailto:margi.hartanto@wur.nl);

Harm Nijveen, Droevendaalsesteeg 1 6708PB WAGENINGEN, phone number:  
+31317484706 , email: [harm.nijveen@wur.nl](mailto:harm.nijveen@wur.nl)

## **Abstract**

Seed germination is characterized by a constant change of gene expression across different time points. These changes are related to specific processes, which eventually determine the onset of seed germination. To get a better understanding on the regulation of gene expression during seed germination, we performed a quantitative trait locus mapping of gene expression (eQTL) at four important seed germination stages (primary dormant, after-ripened, six-hour after imbibition, and radicle protrusion stage) using *Arabidopsis thaliana* Bay x Sha recombinant inbred lines (RILs). The mapping displayed the distinctness of the eQTL landscape for each stage. We found several eQTL hotspots across stages associated with the regulation of expression of a large number of genes. Interestingly, an eQTL hotspot on chromosome five collocates with hotspots for phenotypic and metabolic QTLs in the same population. Finally, we constructed a gene co-expression network to prioritize the regulatory genes for two major eQTL hotspots. The network analysis prioritizes transcription factors DEWAX and ICE1 as the most likely regulatory genes for the hotspot. Together, we have

revealed that the genetic regulation of gene expression is dynamic along the course of seed germination.

## INTRODUCTION

Seed germination involves a series of events starting with the transition of *quiescent* to physiologically active seeds and ends with the emergence of the embryo from its surrounding tissues. Germination is initiated when seeds become imbibed by water, leading to the activation of seed physiological activities (Bewley et al. 2013b; Nonogaki et al. 2010). Major metabolic activities occur after seeds become hydrated, for example, restoration of structural integrity, mitochondrial repair, initiation of respiration, and DNA repair (Bewley et al. 2013b; Nonogaki et al. 2010). For some species such as *Arabidopsis thaliana*, germination can be blocked by seed dormancy. Dormant seeds need to sense and respond to environmental cues to break their dormancy and complete germination. In *Arabidopsis thaliana*, seed dormancy can be alleviated by periods of dry after-ripening or moist chilling (Bewley et al. 2013b). Soon after dormancy is broken, the storage reserves are broken down, and germination-associated proteins are synthesized. Lastly, further water uptake followed by cell expansion leads to radicle protrusion through endosperm and seed coat, which marks the end of germination (Bewley et al. 2013b).

A major determinant for the completion of seed germination is the transcription and translation of mRNAs. The activity of mRNA transcription is low in dry, mature seeds (Comai and Harada 1990; Leubner-Metzger 2005), and drastically increases after seeds become rehydrated (Bewley et al. 2013a). Nevertheless, stored mRNAs of more than 12,000 genes with various functions are already present in dry seeds. These mRNAs are not only remnants from the seed developmental process, but also mRNAs for genes related to metabolism as well as protein synthesis and degradation required in early seed germination (Nakabayashi et al. 2005; Rajjou et al. 2004). Later in after-ripened seeds, only a slight

change in transcript composition was detected compared to the dry seeds (Finch-Savage et al. 2007). The major shift in transcriptome takes place after water imbibition (Nakabayashi et al. 2005). Interestingly, the transcriptome at the imbibition stage depends on the status of dormancy. For non-dormant seeds, most of the transcripts are associated with protein synthesis, while for dormant seeds, the transcripts are dominated by genes associated with stress-responses (Finch-Savage et al. 2007; Buijs et al. 2019). Even the transcript composition in primary dormant seeds, which occurs when the dormancy is initiated during development, is different from that of secondary dormant seeds, which occurs when the dormancy is reinduced (Cadman et al. 2006). These findings show the occurrence of phase transitions in transcript composition along the course from dormant to germinated seed.

As omics technology becomes more widely available, several transcriptomics studies in seed germination processes have been conducted on a larger-scale. More developmental stages, i.e., stratification and seedling stage, and even spatial analyses have been included in these studies, resulting in the identification of gene co-expression patterns as well as the predicted functions of hub-genes (Narsai et al. 2011; Silva et al. 2016; Dekkers et al. 2013; Bassel et al. 2011). Through guilt-by-association, these co-expression based studies can be used for the identification of regulatory genes that are involved in controlling the expression of downstream genes. These regulatory genes can be subjected to further studies by reverse genetics to provide more insight into the molecular mechanisms of gene expression in seed germination (i.e., Silva et al. 2016). Nevertheless, this approach still has limitations. Uygun et al. (2016) argued that co-expressed genes do not always have similar biological functions. On the other hand, genes involved in the same function are not always co-expressed since gene expression regulation could be the result of post-transcriptional or other layers of regulation (Lelli et al. 2012). Further, Uygun et al. (2016) emphasized the importance of combining the

expression data with multiple relevant datasets to maximize the effort in the prioritization of candidate regulatory genes.

Genetical genomics is a promising approach to study the regulation of gene expression by combining genome-wide expression data with genotypic data of a segregating population (Jansen and Nap 2001). To enable this strategy, the location of markers associated with variation in gene expression is mapped on the genome, which results in the identification of expression quantitative trait loci (eQTLs). Relative to the location of the associated gene, the eQTL can be locally or distantly mapped, known as local and distant eQTLs (Rockman and Kruglyak 2006; Brem et al. 2002). Local eQTLs mostly arise because of variations in the corresponding gene or a cis-regulatory element. In contrast, distant eQTLs typically occur due to polymorphism on trans-regulatory elements located far away from the target genes (Rockman and Kruglyak 2006). Therefore, given the positional information of distant eQTLs, one can identify the possible regulators of gene expression. However, the eQTL interval typically spans a large area of the genome and harbors hundreds of candidate regulatory genes. A large number of candidate genes would cause the experimental validation (e.g. using knockout or overexpression lines) to be costly and take a long time. Therefore, a prioritization method is needed to narrow down the list of candidate genes underlying eQTLs, particularly on distant eQTL hotspots. A distant eQTL hotspot is a genomic locus where a large number of distant eQTLs are collocated (Breitling et al. 2008). The common assumption is that the hotspot arises due to one or more polymorphic master regulatory genes affecting the expression of multiple target genes (Breitling et al. 2008). Therefore, the identification of master regulatory genes becomes the center of most genetical genomics studies as the findings might improve our understanding of the regulation of gene expression (i.e., in Keurentjes et al. 2007; Jimenez-Gomez et al. 2010; Sterken et al. 2017; Valba et al. 2015; Terpstra et al. 2010).

In this study, we carried out eQTL mapping to reveal loci controlling gene expression in seed germination. To capture whole transcriptome changes during seed germination, we included four important seed germination stages, which are primary dormant seeds (PD), after-ripened seeds (AR), six-hours imbibed seeds (IM), and seeds with radicle protrusion (RP). In total, 160 recombinant inbred lines (RILs) from a cross between genetically distant ecotypes Bay-0 and Shahdara (Bay x Sha) were used in this study (Loudet et al. 2002). Our results show that each seed germination stage has a unique eQTL landscape, confirming the stage-specificity of gene regulation, particularly for distant regulation. Based on network analysis, we identify the transcription factors ICE1 and DEWAX as prioritized candidate regulatory genes for two major eQTL hotspots in PD and RP, respectively. Finally, the resulting dataset complements the previous phenotypic QTL (Joosen et al. 2012) and metabolite QTL (Joosen et al. 2013) datasets, allowing systems genetics studies in seed germination. The identified eQTLs are available through the web-based AraQTL (<http://www.bioinformatics.nl/AraQTL/>) workbench (Nijveen et al. 2017).

## MATERIALS AND METHODS

### Plant materials

In this study, we used 164 recombinant inbred lines (RILs) derived from a cross between the Bay-0 and Shahdara Arabidopsis ecotypes (Loudet et al. 2002) provided by the Versailles Biological Resource Centre for Arabidopsis (<http://dbsgap.versailles.inra.fr/vnat>). The plants were sown in a fully randomized setup on 4x4 cm rockwool plugs (MM40/40, Groudan B. V.) and hydrated with 1 g/l Hyponex (NPK = 7:6:19, <http://www.hyponex.co.jp>) in a climate chamber (20°C day, 18°C night) with 16 hours of light (35 W/m<sup>2</sup>) at 70% relative humidity. Seeds from four to seven plants per RIL were bulk harvested for the experiment (see also

Joosen et al. 2012; Joosen et al. 2013). The genotypic data consisting of 1,059 markers per line was obtained from Serin et al. (2017). However, the genotypic data is available only for 160 RILs; therefore, we used this number of lines for eQTL mapping.

## **Experimental setup**

The RIL population was grouped into four subpopulations, each one representing one of the four different seed germination stages. We used the designGG-package (Li et al. 2009) in R (version 3.6.0 Windows x64) to aid the grouping so that the distribution of Bay-0 and Sha alleles between sub-populations is optimized. The first stage is the primary dormant (PD) stage when the seeds were harvested and stored at -80°C after one week at ambient conditions. The second stage is after-ripened (AR) seeds that obtained maximum germination potential after five days of imbibition by storing at room temperature and ambient relative humidity. The third stage is the 6 hours imbibition (IM) stage. For this stage, the seeds were after-ripened and imbibed for six hours on water-saturated filter paper at 20°C and immediately transferred to a dry filter paper for 1 minute to remove the excess of water. The fourth stage is the radicle protrusion (RP) stage. To select seeds at this stage, we used a binocular to observe the presence of a protruded radicle tip.

## **RNA isolation**

Total RNA was extracted according to the hot borate protocol modified from Wan and Wilkins (1994). For each treatment, 20 mg of seeds were homogenized and mixed with 800 µl of extraction buffer (0.2M Na boratedecahydrate (Borax), 30 mM EGTA, 1% SDS, 1% Na deoxycholate (Na-DOC)) containing 1.6 mg DTT and 48 mg PVP40 which had been heated to 80°C. Then, 1 mg proteinase K was added to this suspension and incubated for 15 min at 42°C. After adding 64 µl of 2 M KCL, the samples were incubated on ice for 30 min and

subsequently centrifuged for 20 min at 12,000 g. Ice-cold 8 M LiCl was added to the supernatant in a final concentration of 2 M, and the tubes were incubated overnight on ice. After centrifugation for 20 min at 12,000 g at 4°C, the pellets were washed with 750 µl ice-cold 2 M LiCl. The samples were centrifuged for another 10 min at 10,000 g at 4°C, and the pellets were re-suspended in 100 µl DEPC treated water. The samples were phenol-chloroform extracted, DNase treated (RQ1 DNase, Promega), and further purified with RNeasy spin columns (Qiagen) following the manufacturer's instructions. The RNA quality and concentration were assessed by agarose gel electrophoresis and UV spectrophotometry.

## **Microarray analysis**

RNA was processed for use on Affymetrix Arabidopsis SNPtile array (atSNPtilx520433), as described by the manufacturer. Briefly, 1 mg of total RNA was reverse transcribed using a T7-Oligo(dT) Promoter Primer in the first-strand cDNA synthesis reaction. Following RNase H-mediated second-strand cDNA synthesis, the double-stranded cDNA was purified and served as a template in the subsequent in vitro transcription reaction. The reaction was carried out in the presence of T7 RNA polymerase and a biotinylated nucleotide analog/ribonucleotide mix for complementary RNA (cRNA) amplification and biotin labeling. The biotinylated cRNA targets were then cleaned up, fragmented, and hybridized to the SNPtile array. The hybridization data were extracted using a custom R script with the help of an annotation-file based on TAIR10. Intensity data were log-transformed and normalized using the *normalizeBetweenArrays* function with the quantile method from Bioconductor package limma (Ritchie et al. 2015). Then, for each annotated gene, the log-intensities of anti-sense exon probes were averaged.

## **Clustering analysis**

Principal component analysis for log-intensities of all parents and RIL population samples was done using the `pr.comp` function in R where the unscaled log intensities are shifted to be zero centered. For hierarchical clustering, we only selected genes with a minimal fold change of 2 between any pair of consecutive stages (PD to AR, AR to IM, or IM to RP). Then, the distance matrices of filtered genes and all samples were calculated using the absolute Pearson correlation. These matrices were clustered using Ward's method. We manually set the number of clusters to 8 and performed gene ontology enrichment for each of the clusters using the weight algorithm of the `topGO` package in R and used 29,913 genes detected by hybridization probes as the background (Alexa et al. 2006).

## **eQTL mapping**

For eQTL mapping, we used 160 RILs separated into four subpopulations, each representing one specific seed germination stage. For each stage separately, eQTLs were mapped using a single-marker model, as in Sterken et al. (2017). The gene expression data were fitted to the linear model

$$y_{i,j} \sim x_j + e_j$$

where  $y$  is the log-intensity representing the expression of a gene  $i$  ( $i = 1, 2, \dots, 29,913$ ) of RIL  $j$  ( $j = 1, 2, \dots, 160$ ) explained by the parental allele on marker location  $x$  ( $x = 1, 2, \dots, 1,059$ ). The random error in the model is represented by  $e_j$ .

To account for the multiple-testing burden in this analysis, we determined the genome-wide significant threshold using a permutation approach (e.g. see Sterken et al. 2017). A permuted dataset was created by randomly distributing the log-intensities of the gene under study over the genotypes. Then, the previous eQTL mapping model was performed on this permuted dataset. This procedure was repeated 100 times for each stage. The threshold was determined using:

$$\frac{\text{FDS}}{\text{RDS}} \leq \frac{m_0}{m} q \cdot \log(m),$$

where, at a specific significance level, the false discoveries (FDS) were the averaged permutation result, and real discoveries (RDS) were the outcome of the eQTL mapping using the unpermuted dataset. The number of true hypotheses tested ( $m_0$ ) was 29,913 - RDS, and the number of hypotheses ( $m$ ) tested was the number of genes, which was 29,913. For the  $q$ -value, we used a threshold of 0.05. As a result, we got a threshold of 4.2 for PD and AR, 4.1 for IM, and 4.3 for RP.

The confidence interval of an eQTL was determined based on a  $-\log_{10}(p\text{-value})$  drop of 1.5 compared to the peak marker (as in Keurentjes et al. 2007; Cubillos et al. 2012). We determine an eQTL as local if the peak marker or the confidence interval lies within 1 Mb or less from the target gene location (as in Cubillos et al. 2012). All eQTLs that did not meet this criterion were defined as distant.

We defined a region as an eQTL hotspot if the number of distant-eQTLs mapped to a particular genomic region significantly exceeded the expectation. First, we divided the genome into bins of 2 Mb. Then, we determined the expected number of distant-eQTLs per genomic bin by dividing the total number of distant-eQTLs by the total number of bins. Based on a Poisson distribution, any bin having an actual number of distant-eQTLs larger than expected ( $p < 0.0001$ ) was then considered as an eQTL hotspot.

## **Gene regulatory network inference and candidate genes prioritization of eQTL hotspot**

We used a community-based approach to infer regulatory networks of genes with an eQTL on a hotspot location using expression data. In this approach, we assume the hotspot is caused by a polymorphism in or near one or more regulatory genes causing altered expression that can

be detected as a local eQTL (Joosen et al. 2009; Breitling et al. 2008; Jimenez-Gomez et al. 2010; Serin et al. 2017). Based on this assumption, we labeled all genes with a local eQTL on a hotspot as candidate regulators and genes with a distant eQTL as targets. The expression of these genes was subjected to five different network inference methods to predict the interaction weight. The methods used were TIGRESS (Haury et al. 2012), Spearman correlation, CLR (Faith et al. 2007), ARACNE (Margolin et al. 2006), and GENIE3 (Huynh-Thu et al. 2010). The predictions from GENIE3 were used to establish the direction of the interaction by removing the one that has the lowest variable importance to the expression of the target genes between two pairs of genes. For instance, if the importance of  $\text{gene}_i - \text{gene}_j$  is smaller than  $\text{gene}_j - \text{gene}_i$ , then the former is removed. By averaging the rank, the predictions of all inference methods were integrated to produce a robust and high performance prediction (Marbach et al. 2012). The threshold was determined as the minimum average rank where all nodes are included in the network. Finally, the network was visualized using Cytoscape (version 3.7.1) (Shannon et al. 2003), and network properties were calculated using the NetworkAnalyzer tool (Assenov et al. 2008). The candidate genes for each eQTL hotspot were prioritized based on their outdegree and closeness centrality (Pavlopoulos et al. 2011).

## **Data availability**

The list of genetic markers, genotype, and gene expression data used in this study are given in Table S7, Table S8, and Table S9, respectively. Cel files of microarray data have been deposited in the ArrayExpress database at EMBL-EBI ([www.ebi.ac.uk/arrayexpress](http://www.ebi.ac.uk/arrayexpress)) under accession number E-MTAB-9080. The phenotype and metabolite measurement can be found in Table S10 and Table S11. The list of differentially expressed genes is in Table S12. All QTL mapping results are given in Table S13 (expression QTL), Table S14 (phenotype QTL), and Table S15 (metabolite QTL). The code for the analysis and visualization is available in

the form of R scripts at the Wageningen University GitLab repository (<https://git.wur.nl/harta003/seed-germination-qtl>).

## RESULTS

### **Major transcriptional shifts take place after water imbibition and radicle protrusion**

To visualize the transcriptional states of the parental lines and the RILs at the four seed germination stages, we performed a principal component analysis using the log-intensities of all expressed genes (Figure 1). The first principal component explains 55.6% of the variation and separates the samples into three groups. Germination progresses from left to right with the PD and AR seeds grouping together, indicating that the after-ripening treatment does not induce a considerable change in global transcript abundance. The large-scale transcriptome change only happens after water imbibition and radicle protrusion. This event was also observed by Finch-Savage et al. (2007) and Silva et al. (2016). The second principal component on the PCA explains 14.2% variance in the data and separates the RILs within each of the three clusters but not the parents. The source of this variation may be the genetic variation among samples and shows transgressive segregation of gene expression in RILs due to genetic reshuffling of the parental genomes during crossing and generations of selfing.

To identify specific expression patterns among genes in the course of seed germination, we performed an additional analysis of the transcriptome data using hierarchical clustering (Figure 2). For this analysis, we only selected the 990 genes with a minimal fold change of two between any two consecutive stages (PD to AR, AR to IM, IM to RP). We then clustered both the genes and the seed samples. As shown in the figure, the clustering of samples shows

similar grouping as in the previous PCA plot; three clusters were formed with one cluster containing both PD and AR, while IM and RP form separate clusters.

The clustering of genes shows at least three distinctive gene expression patterns. In the first pattern, transcript abundance is highest in the last stage, radicle protrusion. A GO enrichment test suggests that transcripts with this expression pattern are involved in the transition from the heterotrophic seed to the autotrophic seedling stage, with enriched processes such as photosynthesis, response to various light, and response to temperature. This is in agreement with Rajjou et al. (2004), who showed that genes required for seedling growth are expressed after water imbibition. The second pattern shows an opposite trend with higher transcript abundances in the first three stages and lower expression at the end of the seed germination process. Some of these transcripts may be the remnant of seed development since the GO term related to this process is overrepresented. Moreover, transcripts involved in response to hydrogen peroxide were also overrepresented, which provides more evidence for the importance of reactive oxygen species in seed germination (for review see Wojtyla et al. 2016). The last pattern represents genes that are upregulated at the IM stage. Genes with this pattern are functionally enriched in the catabolism of fatty acids, a likely source of energy for seedling growth (Bewley et al. 2013c). Altogether, these results suggest that co-expression patterns of genes reflect particular functions during the seed germination process.

### **Distant eQTLs explain less variance than local eQTLs and are more specific to a seed germination stage**

To map loci associated with gene expression levels, we performed eQTL mapping of 29,913 genes for each seed population representing four seed germination stages (Table 1). We found eQTLs, numbers ranging from 1,335 to 1,719 per stage (FDR = 0.05), spread across the

genome. Among the genes with an eQTL, only a few (less than 1%) had more than one. We then categorized the eQTLs into local and distant based on the distance between the target gene and the eQTL peak marker or the confidence interval. Based on this criterion, over 72% of the eQTLs per stage were categorized as local (located within 1 Mb of the gene), while the remainder were distant. Although the total of the identified eQTLs was different between the stages, the ratio of distant to local eQTLs was relatively similar for all stages. We then calculated the fraction of the total variation that is explained by the simple linear regression model for each eQTL. By comparing the density distributions (Figure S1), we showed that local eQTLs generally explain a more substantial fraction of gene expression variation than distant eQTLs. Finally, we determined the number of specific and shared eQTLs across stages (Figure 3). Here, we show that distant eQTLs are more specific to seed germination stages. Local eQTLs, on the other hand, are commonly shared between two or more stages, which is in line with previous experiments showing overlapping local eQTLs and specific distant eQTLs across different developmental stages (Vinuela et al. 2010), environments (Snoek et al. 2012; Snoek et al. 2017; Lowry et al. 2013) and populations (Cubillos et al. 2012).

### **An eQTL hotspot on chromosome 5 is associated with genes related to seed germination and collocates with multiple metabolic and phenotypic QTLs**

To get an overview of how the eQTLs were mapped over the genome, we visualized the eQTL locations and their associated genes on a local/distant eQTL plot (Figure 4A). Here, the local eQTLs are aligned across the diagonal and spread relatively equally across the genome, while it is not the case for the distant eQTLs. Furthermore, specific loci show clustering of eQTLs, which could indicate the presence of major regulatory genes that cause genome-wide gene expression changes. We identified ten so-called (distant-) eQTL hotspots, with at least two hotspots per stage (Table 2). The number of distant eQTLs located within these hotspots

ranges from 16 to 96. The major eQTL hotspots are PD2, IM2, and RP4, with 69, 69, and 96 distant eQTLs co-locating, respectively. Moreover, the landscape of the eQTL hotspots (Figure 4B) differs for every stage, including PD and AR, which is surprising since these two stages have a relatively similar transcriptome profile (Figure 1).

We remapped the QTLs for previously studied seed germination phenotypes (Joosen et al. 2012) and metabolites (Joosen et al. 2013) using the RNA-seq based genetic map (Serin et al. 2017). We then visualized the resulting QTL count histograms alongside the eQTL histogram (Figure 5). The histogram shows that several eQTL hotspots collocate with hotspots for phenotype and metabolite QTLs (phQTLs and mQTLs, respectively). The most striking example is the collocation of QTLs on chromosome 5 around 24—25 Mb (IM2 and RP4) at the last two stages of seed germination. We performed gene ontology (GO) term enrichment analysis for genes with an eQTL mapping to these hotspots, and found ‘seed germination’ enriched among other terms (Table 2). These findings taken together indicate that the IM2 and RP4 hotspots harbor one or more important genes affecting gene expression during seed germination. Therefore, the identification of the regulatory gene(s) for one of these hotspots can give us more insight into the trans-regulation of gene expression during seed germination.

### **Transcription factors were prioritized as the candidate genes for major eQTL hotspots**

To prioritize the candidate regulatory genes underlying eQTL hotspots in this study, we constructed a network based on the expression of genes with eQTLs on the hotspot location. We built the network for two hotspots: RP4, where QTLs for expression, metabolite, and phenotype are collocated; and PD2, another major eQTL hotspot in this study. For RP4, the total number of genes used to construct the network was 116, of which 20 had a local eQTL at the hotspot, whereas for PD2, 114 genes were identified, of which 45 with a local eQTL. The genes with local eQTLs were then labeled as candidates. The networks were constructed by

integrating predictions from several gene regulatory network inference methods to ensure the robustness of the result (Marbach et al. 2012). The direction of the edges in the network is predicted using the GENIE3 method (Huynh-Thu et al. 2010). For each candidate gene, we calculated the outdegree, indicating the number of outgoing edges of a gene to other genes in the network, and the closeness centrality of the candidate gene nodes, which shows the efficiency of the gene in spreading information to the rest of the genes in the network (Pavlopoulos et al. 2011). Finally, these two network properties were used to prioritize the most likely regulator of the distant eQTL hotspot.

In the resulting network, genes encoding the transcription factors DECREASE WAX BIOSYNTHESIS/DEWAX (AT5G61590), and INDUCER OF CBP EXPRESSION 1/ICE1 (AT3G26744) were prioritized as the most likely candidate genes for RP4 (Figure 6) and PD2 (Figure 7), respectively. As many as 15 genes were predicted to be associated with DEWAX and 32 genes with ICE1. Note that these numbers depend on the chosen threshold; nonetheless, the current candidates are robust to changes when the parameter was changed (Table S3 and Table S4). Furthermore, these two genes also had the highest closeness centrality among the other candidates, showing that these genes have a strong influence within the network. We assessed the Bay x Sha SNP data (Genomes Consortium. Electronic address and Genomes 2016) and found several SNPs between the Bay and Sha parents in both the DEWAX and ICE1 genes, including two that affect the amino acid sequence of the corresponding proteins (Table S5 and Table S6). Also, querying for DEWAX and ICE1 on AraQTL showed a local eQTL for both genes in an experiment using the same RIL population on leaf tissue (West et al. 2007). This evidence supports the hypothesis that polymorphisms between the Bay and Sha alleles of DEWAX and ICE1 are responsible for the steadily occurring local eQTLs at three stages (PD, IM, RP) for DEWAX and all four stages for ICE1.

## DISCUSSION

### **The function of DEWAX may be related to seed cuticular wax biosynthesis**

In this study, we constructed a network of genes associated with the RP4 eQTL hotspot and showed that *DEWAX* was prioritized as the candidate gene for the hotspot. *DEWAX* encodes an AP2/ERF-type transcription factor that is well-known as a negative regulator of cuticular wax biosynthesis (Go et al., 2014; Suh and Go, 2014; Cui et al., 2016; Li et al., 2019) and a positive regulator of defense response against biotic stress (Froschel et al. 2019; Ju et al. 2017). This gene also seems to be involved in drought stress response (Huang et al. 2008) by inducing the expression of genes that confer drought tolerance (Sun et al. 2016), some of which (*LEA4-5*, *LTI-78*) have a distant eQTL at the RP4 hotspot. Moreover, the overexpression of *DEWAX* in *Arabidopsis* increases the seed germination rate (Sun et al. 2016). The role of *DEWAX* in seed germination is still unknown but may be related to cuticular wax biosynthesis.

Wax is a mixture of hydrophobic lipids, which is part of the plant cuticle together with cutin and suberin (Yeats and Rose 2013). Previous studies have demonstrated that the biosynthesis of wax in the cuticular layer of stems and leaves is negatively regulated by *DEWAX* (Go et al., 2014; Suh and Go, 2014; Cui et al., 2016; Li et al., 2019). Although the function of this gene has never been reported in seeds, the presence of a cuticular layer indeed plays a significant role in maintaining seed dormancy (Nonogaki 2019; De Giorgi et al. 2015). In *Arabidopsis* seeds, the thick cuticular structure covering the endosperm prevents cell expansion and testa rupture that precede radicle protrusion. Besides, this layer also reduces the diffusion of oxygen into the seed, thus preventing oxidative stress that may cause rapid seed aging and loss of dormancy (De Giorgi et al. 2015).

Besides *DEWAX*, *MUM2* is another possible regulatory gene for the RP4 hotspot based on QTL confirmation of an imbibed seed size phenotype using a heterogeneous inbred family approach (Joosen et al. 2012). In our study, we also discovered that most eQTLs on the RP4 hotspot peak at the marker located closely to the *MUM2* location (Figure S2), which provides more evidence for this gene as the regulator for the hotspot. *MUM2* encodes a cell-wall modifying beta-galactosidase involved in seed coat mucilage biosynthesis, and the *mum2* mutant is characterized by a failure in extruding mucilage after water imbibition (Dean et al. 2007). In our analysis, *MUM2* did not have a distant eQTL on the RP4 hotspot; thus, it is not prioritized as a prominent candidate, pointing out a limitation of our approach in prioritizing candidate eQTL hotspot genes which will be discussed later. Nonetheless, we found some evidence connecting *DEWAX* to *MUM2*. First, Shi et al. (2019) found out that the mutant of *CPL2*, another gene involved in wax biosynthesis, showed a delayed secretion of the enzyme encoded by *MUM2* that disrupts seed coat mucilage extrusion. In the same study, they revealed that *CPL2* encodes a phosphatase involved in secretory protein trafficking required for the secretion of extracellular matrix materials, including wax and the cell wall-modifying enzyme *MUM2*. Although no direct connection between *DEWAX* and *CPL2* has been reported, a recent study by Xu et al. did identify *DEWAX* as a putative regulator of cell-wall-loosening *EXPANSIN (EXPA)* genes involved in germination (Xu et al. 2020). These findings provide a link between wax biosynthesis and cell-wall modifying enzymes, and possibly between the genes involved in these processes.

Second, the expression of *DEWAX* may be the consequence of the disruption of seed mucilage extrusion. Penfield et al. (2001) suggest that seed mucilage helps enhance water uptake to ensure efficient germination in the condition of low water potential. This is supported by the evidence that the mucilage-impaired mutant showed reduced maximum germination only on osmotic polyethylene glycol solutions (Penfield et al. 2001). Therefore, the absence of

mucilage in imbibed seed under low water potential may cause osmotic stress in the seed and, in turn, induce the expression of DEWAX, which is known to play a role in the response of plants against osmotic stress (Sun et al. 2016). If this is the case, then a scenario could be that DEWAX acts downstream of MUM2, and the expression variation of these two genes lead to the emergence of the RP4 eQTL hotspot.

#### **Network analysis shows the involvement of ICE1 as a regulator of gene expression during seed germination**

ICE1 is an MYC-like basic helix-loop-helix (bHLH) transcription factor that shows pleiotropic effects in plants. Earlier studies of ICE1 mostly focus on the protein function in the acquisition of cold tolerance (Lee et al. 2005; Chinnusamy et al. 2003) and stomatal lineage development (Kanaoka et al. 2008). Recently, ICE1 was also shown to form a heterodimer with ZOU, another bHLH transcription factor, to regulate endosperm breakdown required for embryo growth during seed development (Denay et al. 2014). At a later stage, ICE1 negatively regulates ABA-dependent pathways to promote seed germination and seedling establishment (Liang and Yang 2015). This process involves repressing the expression of transcription factors in ABA signaling, such as ABI3 and ABI5, and ABA-responsive genes, such as *EM6* and *EM1*, thus initiating seed germination and subsequent seedling establishment (Hu et al. 2019; MacGregor et al. 2019). Loss of *ice1* has been reported to lead to reduced germination (MacGregor et al., 2019)

In this study, we performed a network analysis for genes having distant eQTLs on the PD2 hotspot and prioritized ICE1 as the most likely regulator using network analysis. The high connectivity of ICE1 with the other genes in the network could reflect an essential regulatory function of this gene during seed germination. However, we did not find any of the known

ICE1 target genes (i.e., *ABI3*, *ABI5*, *EM1*, and *EM6*) nor seed germination phenotype (Figure 5) having an eQTL at the *ICE1* locus. It could be that the ICE1 polymorphism is not severe enough to cause considerable trait variation, especially to break a robust biological system where several buffering mechanisms exist to prevent small molecular perturbation from propagating to the phenotypic level (Signor and Nuzhdin 2018; Fu et al. 2009).

A good strategy to validate that a predicted candidate gene indeed causes a QTL hotspot would be to test one parent's allele of the gene in the genetic background of the other parent. This could be achieved by generating near-isogeneic lines, although rapid developments in site directed mutagenesis might offer a more feasible high-throughput approach for future studies. Next, being able to convert one parent's gene into the other parent's gene one SNP at a time would even allow identification of causal SNPs.

#### **Limitations of co-expression network in identifying candidate genes of eQTL hotspots**

The construction of a co-expression network is a promising approach to prioritize candidate eQTL genes (Serin et al. 2016). Despite its potential, there is a major limitation in using a co-expression network. The network is based on gene expression data; hence the identified causal genes are those that directly affect gene expression. For example, as we described above, our approach did not prioritize *MUM2* for the RP4 hotspot, possibly because the gene does not cause variation in the target gene expression but rather causes differences at another level of target gene regulation (e.g., enzyme biosynthesis) between two parental alleles in the RIL population. Other studies reported similar results where a known causal gene was not detected as a hub in the network (Jimenez-Gomez et al. 2010; Sterken et al. 2017). To overcome this, future work should focus on networks that are built upon multi-omics data by including metabolic, proteomic, and, more importantly, phenotypic measurement data (Hawe et al. 2019). Moreover, prior biological knowledge, including protein-protein interaction (Szklarczyk et al. 2017), transcription factor binding-site (Kulkarni et al. 2018), and other

types of interactions (for review see Kulkarni and Vandepoele 2019) can be incorporated to construct data-driven interaction networks. Nevertheless, our approach offers a simple and straightforward way to prioritize candidate genes underlying eQTL hotspots from a limited amount of resources.

## Tables

**Table 1.** Summary of the eQTL mapping for the four different seed germination stages

stage	eQTLs	genes with an eQTL	eQTL type	total	proportion
<b>primary dormant</b>	1,335	1,328	local	955	0.72
			distant	380	0.28
<b>after-ripened</b>	1,395	1,377	local	1,089	0.78
			distant	306	0.22
<b>six hours after imbibition</b>	1,719	1,702	local	1,320	0.77
			distant	399	0.23
<b>radicle protrusion</b>	1,426	1,418	local	1,096	0.77
			distant	330	0.23

**Table 2.** Distant eQTL hotspots of the four seed germination stages. These hotspots were identified by dividing the genome into bins of 2 Mbp and performing a test to determine whether the number of distant eQTLs on a particular bin is higher than expected ( $p > 0.0001$ ) assuming a Poisson distribution. Seed germination phenotype and metabolite data were taken from Joosen et al. (2012) and Joosen et al. (2013), respectively. Detailed information about enriched GO terms, metabolite, and phenotype can be seen on Supplemental Table S2 in the Supplementary Material.

hotspot ID	position	distant eQTLs	enriched GO terms	metabolite QTL	phenotype QTL
<b>PD1</b>	ch1:6-10 Mb	43	11	1	4
<b>PD2</b>	ch3:8-12 Mb	69	3	2	1
<b>AR1</b>	ch2:12-14 Mb	16	0	0	0
<b>AR2</b>	ch3:2-4 Mb	20	9	1	1

<b>IM1</b>	ch5:6-8 Mb	19	2	24	1
<b>IM2</b>	ch5:22-26 Mb	69	6	6	31
<b>RP1</b>	ch1:0-2 Mb	23	1	0	1
<b>RP2</b>	ch1:6-8 Mb	18	0	0	3
<b>RP3</b>	ch5:14-16 Mb	21	29	0	1
<b>RP4</b>	ch5:24-26Mb	96	18	20	25

## Literature cited

- Alexa, A., J. Rahnenführer, and T. Lengauer, 2006 Improved scoring of functional groups from gene expression data by decorrelating GO graph structure. *Bioinformatics* 22 (13):1600-1607.
- Assenov, Y., F. Ramirez, S.E. Schelhorn, T. Lengauer, and M. Albrecht, 2008 Computing topological parameters of biological networks. *Bioinformatics* 24 (2):282-284.
- Bassel, G.W., H. Lan, E. Glaab, D.J. Gibbs, T. Gerjets *et al.*, 2011 Genome-wide network model capturing seed germination reveals coordinated regulation of plant cellular phase transitions. *Proc Natl Acad Sci U S A* 108 (23):9709-9714.
- Bewley, J.D., K.J. Bradford, H.W.M. Hilhorst, and H. Nonogaki, 2013a Dormancy and the Control of Germination, pp. 247-297 in *Seeds: Physiology of Development, Germination and Dormancy, 3rd Edition*, edited by J.D. Bewley, K.J. Bradford, H.W.M. Hilhorst and H. Nonogaki. Springer New York, New York, NY.
- Bewley, J.D., K.J. Bradford, H.W.M. Hilhorst, and H. Nonogaki, 2013b Germination, pp. 133-181 in *Seeds: Physiology of Development, Germination and Dormancy, 3rd Edition*, edited by J.D. Bewley, K.J. Bradford, H.W.M. Hilhorst and H. Nonogaki. Springer New York, New York, NY.
- Bewley, J.D., K.J. Bradford, H.W.M. Hilhorst, and H. Nonogaki, 2013c Synthesis of Storage Reserves, pp. 85-131 in *Seeds: Physiology of Development, Germination and*

*Dormancy, 3rd Edition*, edited by J.D. Bewley, K.J. Bradford, H.W.M. Hilhorst and H. Nonogaki. Springer New York, New York, NY.

Breitling, R., Y. Li, B.M. Tesson, J. Fu, C. Wu *et al.*, 2008 Genetical genomics: spotlight on QTL hotspots. *PLoS Genet* 4 (10):e1000232.

Brem, R.B., G. Yvert, R. Clinton, and L. Kruglyak, 2002 Genetic dissection of transcriptional regulation in budding yeast. *Science* 296 (5568):752-755.

Buijs, G., A. Vogelzang, H. Nijveen, and L. Bentsink, 2019 Dormancy cycling: Translation related transcripts are the main difference between dormant and non-dormant seeds in the field. *Plant J*.

Cadman, C.S., P.E. Toorop, H.W. Hilhorst, and W.E. Finch-Savage, 2006 Gene expression profiles of Arabidopsis Cvi seeds during dormancy cycling indicate a common underlying dormancy control mechanism. *Plant J* 46 (5):805-822.

Chinnusamy, V., M. Ohta, S. Kanrar, B.H. Lee, X. Hong *et al.*, 2003 ICE1: a regulator of cold-induced transcriptome and freezing tolerance in Arabidopsis. *Genes Dev* 17 (8):1043-1054.

Comai, L., and J.J. Harada, 1990 Transcriptional activities in dry seed nuclei indicate the timing of the transition from embryogeny to germination. *Proc Natl Acad Sci U S A* 87 (7):2671-2674.

Cubillos, F.A., J. Yansouni, H. Khalili, S. Balzergue, S. Elftieh *et al.*, 2012 Expression variation in connected recombinant populations of Arabidopsis thaliana highlights distinct transcriptome architectures. *BMC Genomics* 13:117.

De Giorgi, J., U. Piskurewicz, S. Loubery, A. Utz-Pugin, C. Bailly *et al.*, 2015 An Endosperm-Associated Cuticle Is Required for Arabidopsis Seed Viability, Dormancy and Early Control of Germination. *PLoS Genet* 11 (12):e1005708.

557 Dean, G.H., H. Zheng, J. Tewari, J. Huang, D.S. Young *et al.*, 2007 The Arabidopsis MUM2  
 558 gene encodes a beta-galactosidase required for the production of seed coat mucilage  
 559 with correct hydration properties. *Plant Cell* 19 (12):4007-4021.

560 Dekkers, B.J., S. Pearce, R.P. van Bolderen-Veldkamp, A. Marshall, P. Widera *et al.*, 2013  
 561 Transcriptional dynamics of two seed compartments with opposing roles in  
 562 Arabidopsis seed germination. *Plant Physiol* 163 (1):205-215.

563 Denay, G., A. Creff, S. Moussu, P. Wagnon, J. Thevenin *et al.*, 2014 Endosperm breakdown  
 564 in Arabidopsis requires heterodimers of the basic helix-loop-helix proteins ZHOUP1  
 565 and INDUCER OF CBP EXPRESSION 1. *Development* 141 (6):1222-1227.

566 Faith, J.J., B. Hayete, J.T. Thaden, I. Mogno, J. Wierzbowski *et al.*, 2007 Large-scale  
 567 mapping and validation of Escherichia coli transcriptional regulation from a  
 568 compendium of expression profiles. *PLoS Biol* 5 (1):e8.

569 Finch-Savage, W.E., C.S. Cadman, P.E. Toorop, J.R. Lynn, and H.W. Hilhorst, 2007 Seed  
 570 dormancy release in Arabidopsis Cvi by dry after-ripening, low temperature, nitrate  
 571 and light shows common quantitative patterns of gene expression directed by  
 572 environmentally specific sensing. *Plant J* 51 (1):60-78.

573 Froschel, C., T. Iven, E. Walper, V. Bachmann, C. Weiste *et al.*, 2019 A Gain-of-Function  
 574 Screen Reveals Redundant ERF Transcription Factors Providing Opportunities for  
 575 Resistance Breeding Toward the Vascular Fungal Pathogen Verticillium longisporum.  
 576 *Mol Plant Microbe Interact* 32 (9):1095-1109.

577 Fu, J., J.J. Keurentjes, H. Bouwmeester, T. America, F.W. Verstappen *et al.*, 2009 System-  
 578 wide molecular evidence for phenotypic buffering in Arabidopsis. *Nat Genet* 41  
 579 (2):166-167.

Genomes Consortium. Electronic address, m.n.g.o.a.a., and C. Genomes, 2016 1,135  
 Genomes Reveal the Global Pattern of Polymorphism in *Arabidopsis thaliana*. *Cell*  
 166 (2):481-491.

Haury, A.C., F. Mordelet, P. Vera-Licona, and J.P. Vert, 2012 TIGRESS: Trustful Inference  
 of Gene REgulation using Stability Selection. *BMC Syst Biol* 6:145.

Hawe, J.S., F.J. Theis, and M. Heinig, 2019 Inferring Interaction Networks From Multi-  
 Omics Data. *Front Genet* 10:535.

Hu, Y., X. Han, M. Yang, M. Zhang, J. Pan *et al.*, 2019 The Transcription Factor INDUCER  
 OF CBF EXPRESSION1 Interacts with ABSCISIC ACID INSENSITIVE5 and  
 DELLA Proteins to Fine-Tune Absciscic Acid Signaling during Seed Germination in  
*Arabidopsis*. *Plant Cell* 31 (7):1520-1538.

Huang, D., W. Wu, S.R. Abrams, and A.J. Cutler, 2008 The relationship of drought-related  
 gene expression in *Arabidopsis thaliana* to hormonal and environmental factors. *J Exp*  
*Bot* 59 (11):2991-3007.

Huynh-Thu, V.A., A. Irrthum, L. Wehenkel, and P. Geurts, 2010 Inferring regulatory  
 networks from expression data using tree-based methods. *PLoS One* 5 (9).

Jansen, R., and J. Nap, 2001 Genetical genomics: the added value from segregation. *Trends in*  
*Genetics* 17 (7):388-391.

Jimenez-Gomez, J.M., A.D. Wallace, and J.N. Maloof, 2010 Network analysis identifies  
 ELF3 as a QTL for the shade avoidance response in *Arabidopsis*. *PLoS Genet* 6  
 (9):e1001100.

Joosen, R.V., D. Arends, Y. Li, L.A. Willems, J.J. Keurentjes *et al.*, 2013 Identifying  
 genotype-by-environment interactions in the metabolism of germinating *arabidopsis*  
 seeds using generalized genetical genomics. *Plant Physiol* 162 (2):553-566.

604 Joosen, R.V., D. Arends, L.A. Willems, W. Ligterink, R.C. Jansen *et al.*, 2012 Visualizing the  
605 genetic landscape of Arabidopsis seed performance. *Plant Physiol* 158 (2):570-589.

606 Joosen, R.V., W. Ligterink, H.W. Hilhorst, and J.J. Keurentjes, 2009 Advances in genetical  
607 genomics of plants. *Curr Genomics* 10 (8):540-549.

608 Ju, S., Y.S. Go, H.J. Choi, J.M. Park, and M.C. Suh, 2017 DEWAX Transcription Factor Is  
609 Involved in Resistance to Botrytis cinerea in Arabidopsis thaliana and Camelina  
610 sativa. *Front Plant Sci* 8:1210.

611 Kanaoka, M.M., L.J. Pillitteri, H. Fujii, Y. Yoshida, N.L. Bogenschutz *et al.*, 2008  
612 SCREAM/ICE1 and SCREAM2 specify three cell-state transitional steps leading to  
613 arabidopsis stomatal differentiation. *Plant Cell* 20 (7):1775-1785.

614 Keurentjes, J.J., J. Fu, I.R. Terpstra, J.M. Garcia, G. van den Ackerveken *et al.*, 2007  
615 Regulatory network construction in Arabidopsis by using genome-wide gene  
616 expression quantitative trait loci. *Proc Natl Acad Sci U S A* 104 (5):1708-1713.

617 Kulkarni, S.R., and K. Vandepoele, 2019 Inference of plant gene regulatory networks using  
618 data-driven methods: A practical overview. *Biochim Biophys Acta Gene Regul*  
619 *Mech*:194447.

620 Kulkarni, S.R., D. Vanechoutte, J. Van de Velde, and K. Vandepoele, 2018 TF2Network:  
621 predicting transcription factor regulators and gene regulatory networks in Arabidopsis  
622 using publicly available binding site information. *Nucleic Acids Res* 46 (6):e31.

623 Lee, B.H., D.A. Henderson, and J.K. Zhu, 2005 The Arabidopsis cold-responsive  
624 transcriptome and its regulation by ICE1. *Plant Cell* 17 (11):3155-3175.

625 Lelli, K.M., M. Slattery, and R.S. Mann, 2012 Disentangling the many layers of eukaryotic  
626 transcriptional regulation. *Annu Rev Genet* 46:43-68.

Leubner-Metzger, G., 2005 beta-1,3-Glucanase gene expression in low-hydrated seeds as a mechanism for dormancy release during tobacco after-ripening. *Plant J* 41 (1):133-145.

Li, Y., M.A. Swertz, G. Vera, J. Fu, R. Breitling *et al.*, 2009 designGG: an R-package and web tool for the optimal design of genetical genomics experiments. *BMC Bioinformatics* 10 (1):188.

Liang, C.H., and C.C. Yang, 2015 Identification of ICE1 as a negative regulator of ABA-dependent pathways in seeds and seedlings of Arabidopsis. *Plant Mol Biol* 88 (4-5):459-470.

Loudet, O., S. Chaillou, C. Camilleri, D. Bouchez, and F. Daniel-Vedele, 2002 Bay-0  $\times$  Shahdara recombinant inbred line population: a powerful tool for the genetic dissection of complex traits in Arabidopsis. *Theoretical and Applied Genetics* 104 (6):1173-1184.

Lowry, D.B., T.L. Logan, L. Santuari, C.S. Hardtke, J.H. Richards *et al.*, 2013 Expression quantitative trait locus mapping across water availability environments reveals contrasting associations with genomic features in Arabidopsis. *Plant Cell* 25 (9):3266-3279.

MacGregor, D.R., N. Zhang, M. Iwasaki, M. Chen, A. Dave *et al.*, 2019 ICE1 and ZOU determine the depth of primary seed dormancy in Arabidopsis independently of their role in endosperm development. *Plant J* 98 (2):277-290.

Marbach, D., J.C. Costello, R. Kuffner, N.M. Vega, R.J. Prill *et al.*, 2012 Wisdom of crowds for robust gene network inference. *Nat Methods* 9 (8):796-804.

Margolin, A.A., I. Nemenman, K. Basso, C. Wiggins, G. Stolovitzky *et al.*, 2006 ARACNE: an algorithm for the reconstruction of gene regulatory networks in a mammalian cellular context. *BMC Bioinformatics* 7 Suppl 1:S7.

652 Nakabayashi, K., M. Okamoto, T. Koshiba, Y. Kamiya, and E. Nambara, 2005 Genome-wide  
653 profiling of stored mRNA in *Arabidopsis thaliana* seed germination: epigenetic and  
654 genetic regulation of transcription in seed. *Plant J* 41 (5):697-709.

655 Narsai, R., S.R. Law, C. Carrie, L. Xu, and J. Whelan, 2011 In-depth temporal transcriptome  
656 profiling reveals a crucial developmental switch with roles for RNA processing and  
657 organelle metabolism that are essential for germination in *Arabidopsis*. *Plant Physiol*  
658 157 (3):1342-1362.

659 Nijveen, H., W. Ligterink, J.J. Keurentjes, O. Loudet, J. Long *et al.*, 2017 AraQTL -  
660 workbench and archive for systems genetics in *Arabidopsis thaliana*. *Plant J* 89  
661 (6):1225-1235.

662 Nonogaki, H., 2019 Seed germination and dormancy: The classic story, new puzzles, and  
663 evolution. *J Integr Plant Biol* 61 (5):541-563.

664 Nonogaki, H., G.W. Bassel, and J.D. Bewley, 2010 Germination—Still a mystery. *Plant*  
665 *Science* 179 (6):574-581.

666 Pavlopoulos, G.A., M. Secrier, C.N. Moschopoulos, T.G. Soldatos, S. Kossida *et al.*, 2011  
667 Using graph theory to analyze biological networks. *BioData Min* 4:10.

668 Penfield, S., R.C. Meissner, D.A. Shoue, N.C. Carpita, and M.W. Bevan, 2001 MYB61 Is  
669 Required for Mucilage Deposition and Extrusion in the *Arabidopsis* Seed Coat. *The*  
670 *Plant Cell* 13 (12):2777-2791.

671 Rajjou, L., K. Gallardo, I. Debeaujon, J. Vandekerckhove, C. Job *et al.*, 2004 The effect of  
672 alpha-amanitin on the *Arabidopsis* seed proteome highlights the distinct roles of stored  
673 and neosynthesized mRNAs during germination. *Plant Physiol* 134 (4):1598-1613.

674 Ritchie, M.E., B. Phipson, D. Wu, Y. Hu, C.W. Law *et al.*, 2015 limma powers differential  
675 expression analyses for RNA-sequencing and microarray studies. *Nucleic Acids*  
676 *Research* 43 (7):e47-e47.

Rockman, M.V., and L. Kruglyak, 2006 Genetics of global gene expression. *Nat Rev Genet* 7 (11):862-872.

Serin, E.A., H. Nijveen, H.W. Hilhorst, and W. Ligterink, 2016 Learning from Co-expression Networks: Possibilities and Challenges. *Front Plant Sci* 7:444.

Serin, E.A.R., L.B. Snoek, H. Nijveen, L.A.J. Willems, J.M. Jimenez-Gomez *et al.*, 2017 Construction of a High-Density Genetic Map from RNA-Seq Data for an Arabidopsis Bay-0 x Shahdara RIL Population. *Front Genet* 8:201.

Shannon, P., A. Markiel, O. Ozier, N.S. Baliga, J.T. Wang *et al.*, 2003 Cytoscape: a software environment for integrated models of biomolecular interaction networks. *Genome Res* 13 (11):2498-2504.

Shi, L., G.H. Dean, H. Zheng, M.J. Meents, T.M. Haslam *et al.*, 2019 ECERIFERUM11/C-TERMINAL DOMAIN PHOSPHATASE-LIKE2 Affects Secretory Trafficking. *Plant Physiol* 181 (3):901-915.

Signor, S.A., and S.V. Nuzhdin, 2018 The Evolution of Gene Expression in cis and trans. *Trends Genet* 34 (7):532-544.

Silva, A.T., P.A. Ribone, R.L. Chan, W. Ligterink, and H.W. Hilhorst, 2016 A Predictive Coexpression Network Identifies Novel Genes Controlling the Seed-to-Seedling Phase Transition in Arabidopsis thaliana. *Plant Physiol* 170 (4):2218-2231.

Snoek, B.L., M.G. Sterken, R.P.J. Bevers, R.J.M. Volkers, A. Van't Hof *et al.*, 2017 Contribution of trans regulatory eQTL to cryptic genetic variation in C. elegans. *BMC Genomics* 18 (1):500.

Snoek, L.B., I.R. Terpstra, R. Dekter, G. Van den Ackerveken, and A.J. Peeters, 2012 Genetical Genomics Reveals Large Scale Genotype-By-Environment Interactions in Arabidopsis thaliana. *Front Genet* 3:317.

701 Sterken, M.G., L. van Bemmelen van der Plaat, J.A.G. Riksen, M. Rodriguez, T. Schmid *et*  
 702 *al.*, 2017 Ras/MAPK Modifier Loci Revealed by eQTL in *Caenorhabditis elegans*. *G3*  
 703 *(Bethesda)* 7 (9):3185-3193.

704 Sun, Z.M., M.L. Zhou, W. Dan, Y.X. Tang, M. Lin *et al.*, 2016 Overexpression of the Lotus  
 705 corniculatus Soloist Gene LcAP2/ERF107 Enhances Tolerance to Salt Stress. *Protein*  
 706 *Pept Lett* 23 (5):442-449.

707 Szklarczyk, D., J.H. Morris, H. Cook, M. Kuhn, S. Wyder *et al.*, 2017 The STRING database  
 708 in 2017: quality-controlled protein-protein association networks, made broadly  
 709 accessible. *Nucleic Acids Res* 45 (D1):D362-D368.

710 Terpstra, I.R., L.B. Snoek, J.J. Keurentjes, A.J. Peeters, and G. van den Ackerveken, 2010  
 711 Regulatory network identification by genetical genomics: signaling downstream of the  
 712 Arabidopsis receptor-like kinase ERECTA. *Plant Physiol* 154 (3):1067-1078.

713 Uygun, S., C. Peng, M.D. Lehti-Shiu, R.L. Last, and S.H. Shiu, 2016 Utility and Limitations  
 714 of Using Gene Expression Data to Identify Functional Associations. *PLoS Comput*  
 715 *Biol* 12 (12):e1005244.

716 Valba, O.V., S.K. Nechaev, M.G. Sterken, L.B. Snoek, J.E. Kammenga *et al.*, 2015 On  
 717 predicting regulatory genes by analysis of functional networks in *C. elegans*. *BioData*  
 718 *Min* 8:33.

719 Vinuela, A., L.B. Snoek, J.A. Riksen, and J.E. Kammenga, 2010 Genome-wide gene  
 720 expression regulation as a function of genotype and age in *C. elegans*. *Genome Res* 20  
 721 (7):929-937.

722 Wan, C.Y., and T.A. Wilkins, 1994 A Modified Hot Borate Method Significantly Enhances  
 723 the Yield of High-Quality RNA from Cotton (*Gossypium hirsutum* L.). *Analytical*  
 724 *Biochemistry* 223 (1):7-12.

725 West, M.A., K. Kim, D.J. Kliebenstein, H. van Leeuwen, R.W. Michelmore *et al.*, 2007  
726 Global eQTL mapping reveals the complex genetic architecture of transcript-level  
727 variation in Arabidopsis. *Genetics* 175 (3):1441-1450.

728 Wojtyla, L., K. Lechowska, S. Kubala, and M. Garnczarska, 2016 Different Modes of  
729 Hydrogen Peroxide Action During Seed Germination. *Front Plant Sci* 7:66.

730 Xu, H., O. Lantzouni, T. Bruggink, R. Benjamins, F. Lanfermeijer *et al.*, 2020 A Molecular  
731 Signal Integration Network Underpinning Arabidopsis Seed Germination. *Curr Biol*.

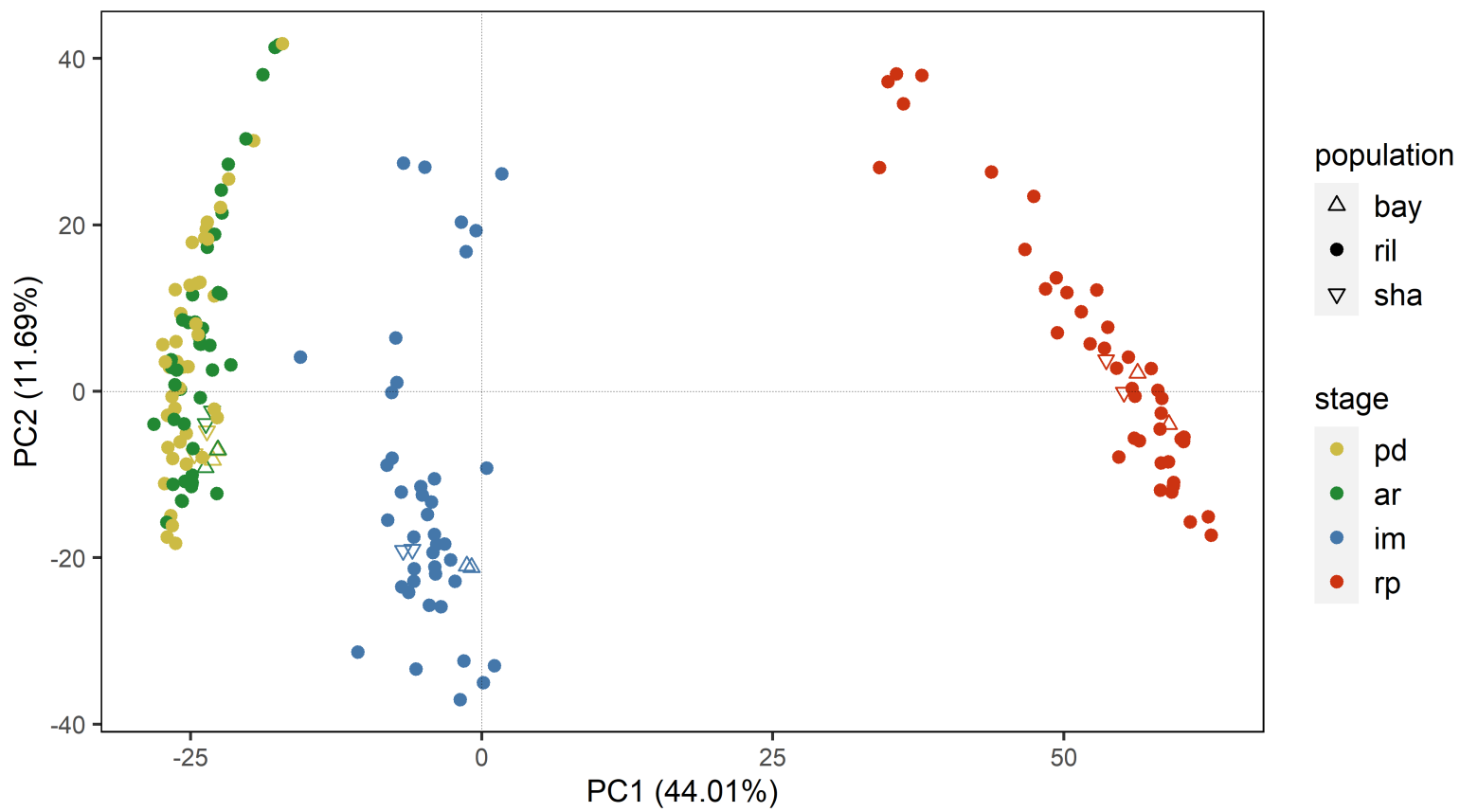
732 Yeats, T.H., and J.K. Rose, 2013 The formation and function of plant cuticles. *Plant Physiol*  
733 163 (1):5-20.

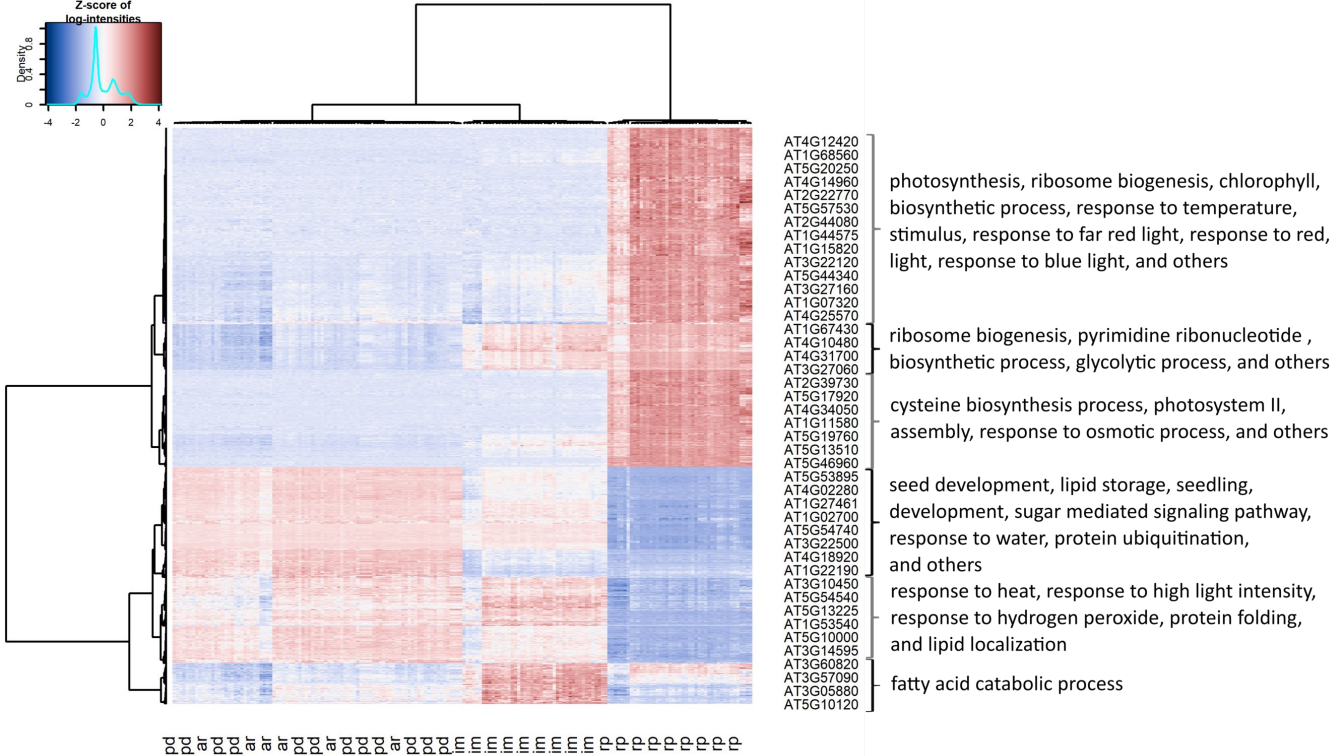
734

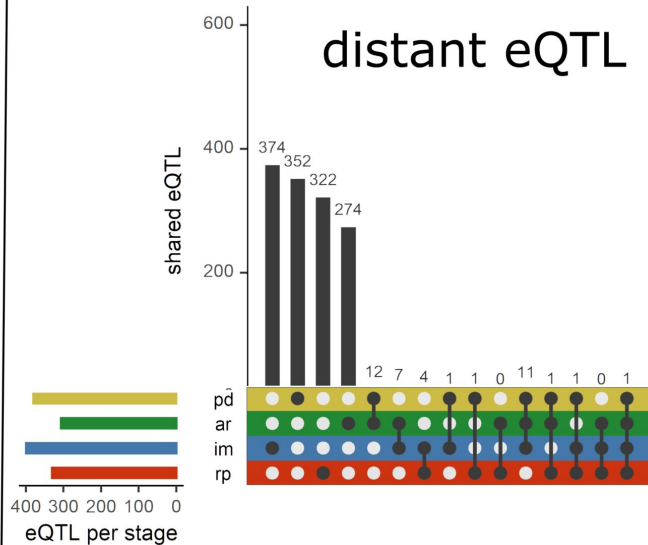
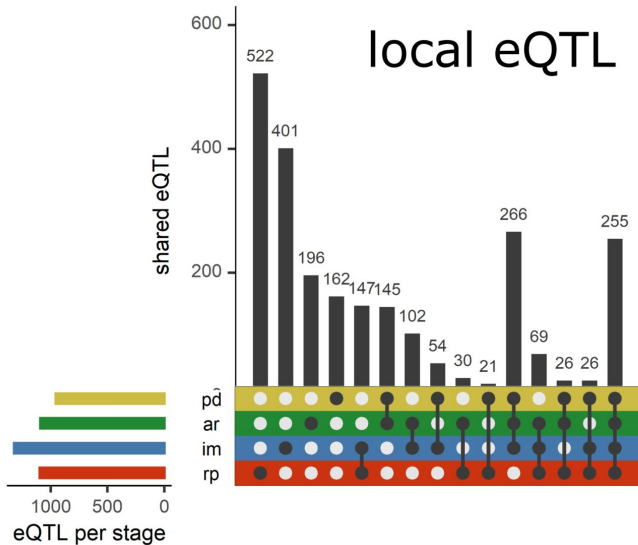
735

736

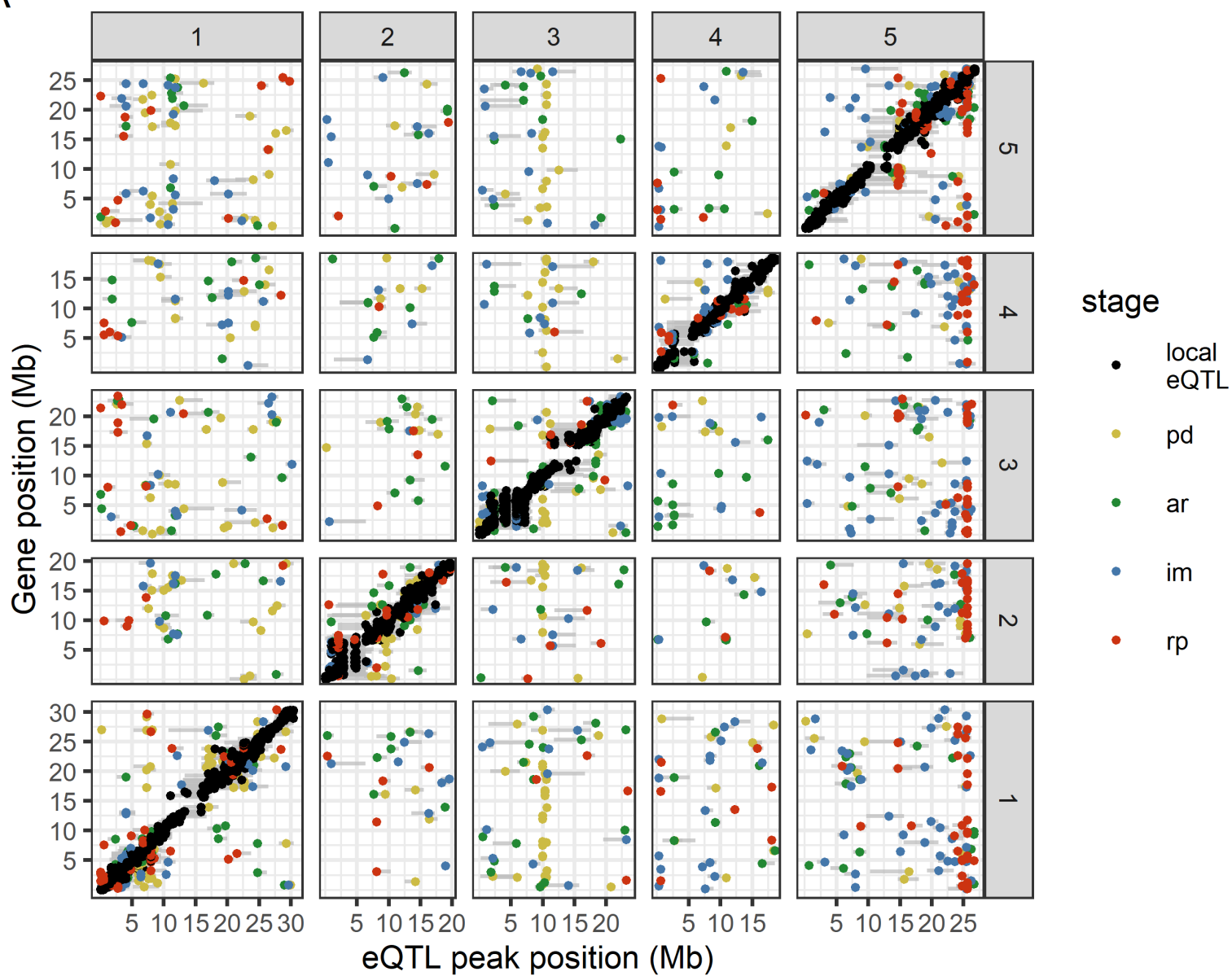
737



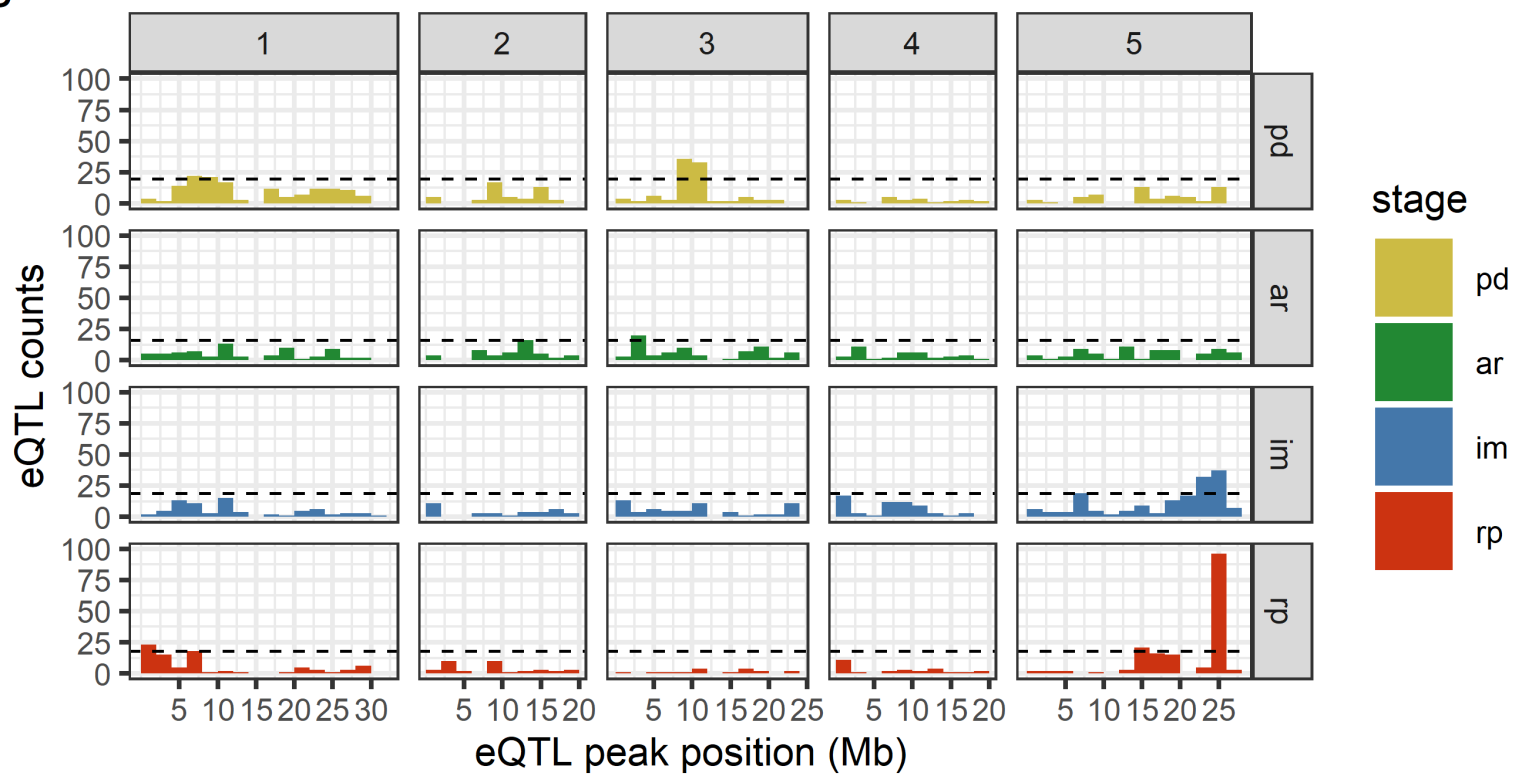


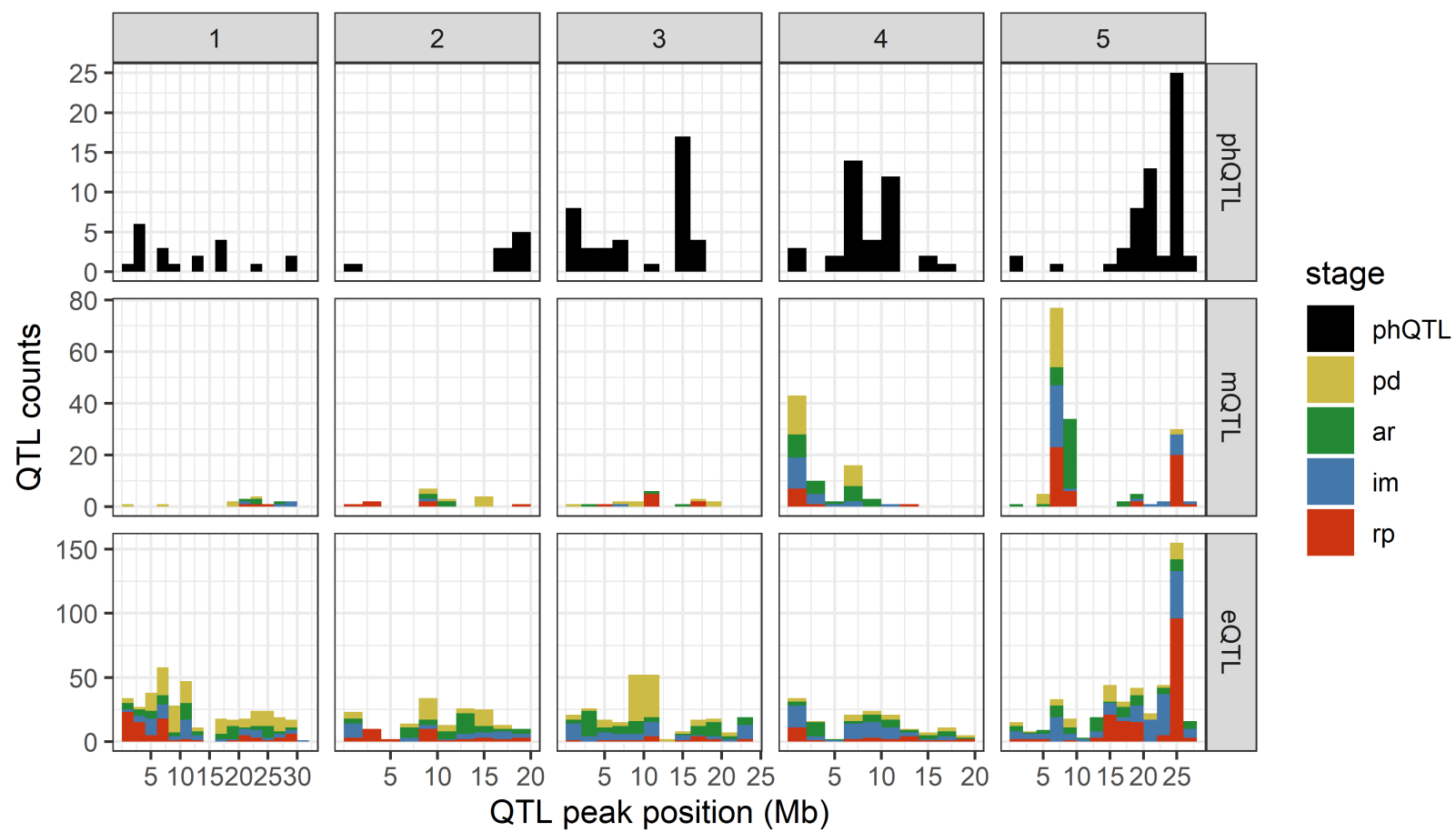


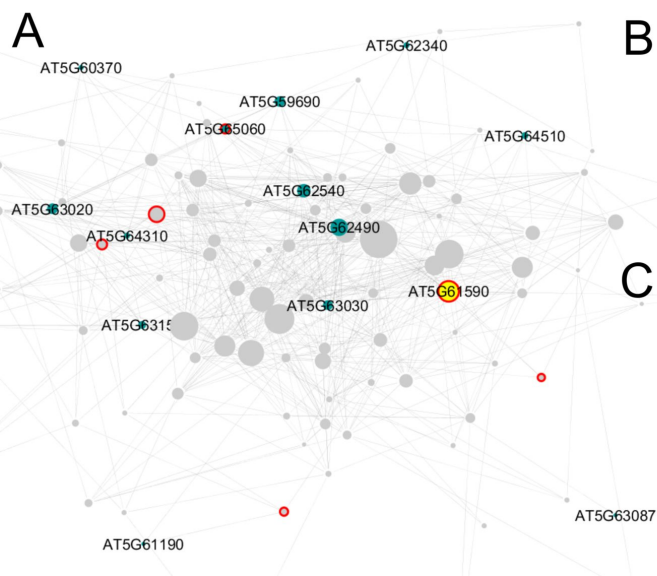
A



B

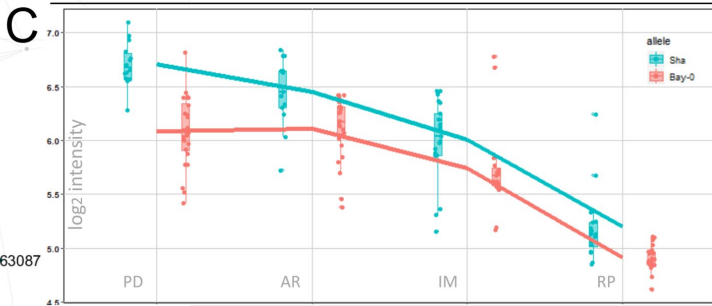


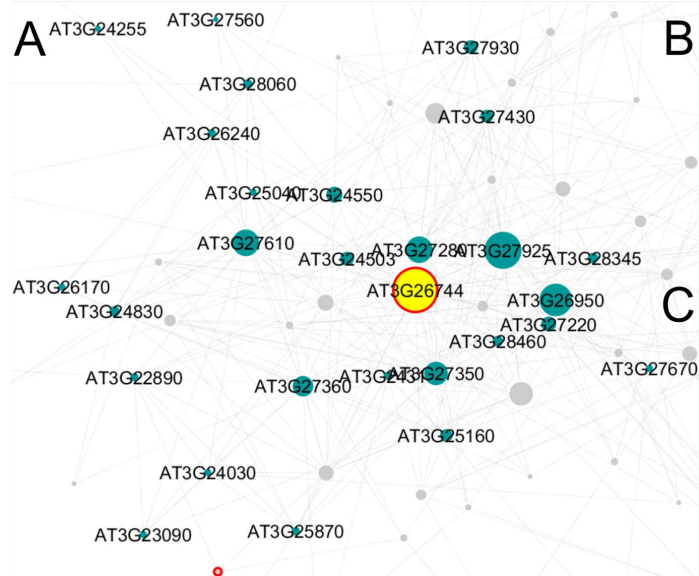




**B**

gene	Out-degree	Closeness Centrality	description
AT5G61590/DEWAX	15	0.45	transcription factor in cutin biosynthesis
AT5G62490/HVA22B	14	0.44	ABA-responsive protein
AT5G62540/UBC3	10	0.41	ubiquitin conjugating enzyme
AT5G59690	7	0.24	histone superfamily protein
AT5G63020/SUT1	7	0.27	NB-LRR mediating immune response
AT5G63030/GRXC1	6	0.25	Thioredoxin superfamily protein
AT5G63150	4	0.23	hypothetical protein
AT5G64510/TIN1	3	0.23	ER stress-inducible protein
AT5G65060/MAF3	3	0.23	MADS-box transcription factor family protein





**B**

gene	Out-degree	Closeness Centrality	description
AT3G26744/ICE1	32	0.54	MYC-like bHLH transcriptional activator
AT3G27925/DEG1	27	0.51	DegP protease
AT3G26950	26	0.46	unknown protein
AT3G27280/PHB4	20	0.46	Prohibitin-4
AT3G27610	18	0.42	Nucleotidyl transferase superfamily protein
AT3G27350	16	0.44	Transcriptional regulator ATRX -like protein
AT3G27360/H3.1	16	0.43	Histone superfamily protein
AT3G24550	13	0.40	Heavy metal transport superfamily protein
AT3G27220/ARI4	9	0.37	IBR domain containing protein
AT3G24503/ALDH1A	8	0.34	Aldehyde dehydrogenase

